Check for updates

Polymers for Advanced Technologies

WILEY

polymers advanced technologies

RESEARCH ARTICLE OPEN ACCESS

Template Assisted Fabrication of Ciprofloxacin-Imprinted Polymers for Removal of Ciprofloxacin

Rashid Mahmood[1] | Showkat Ahmad Bhawani[1] | Rachel Marcella Roland[1] | Syed Rizwan Shafqat[2] | Nadeem A. Khan[3]

[1]Faculty of Resource Science and Technology, Universiti Malaysia Sarawak (UNIMAS), Kota Samarahan, Sarawak, Malaysia | [2]Department of Chemistry, University of Sialkot, Sialkot, Pakistan | [3]Civil Engineering Department, College of Engineering, King Khalid University, Abha, Saudi Arabia

Correspondence: Showkat Ahmad Bhawani (bshowkat@unimas.my)

Received: 27 October 2025 | **Revised:** 16 January 2026 | **Accepted:** 21 January 2026

Keywords: adsorption | batching binding | ciprofloxacin | molecular imprinted polymer | water pollution

ABSTRACT

The study presents the development of highly specific molecular imprinted polymers for adsorptive removal of ciprofloxacin (CIP) from aqueous media. Ciprofloxacin is one of the commonly used antibiotics which is usually found in effluents due to its inadequate removal from wastewater by conventional treatment methods. In aquatic settings, its persistence contributes to antibiotic resistance and hence poses different risks for aquatic organisms. In this study, the removal behavior of CIP designated as a model contaminant was investigated using state of the art Molecular Imprinting Technology (MIT). Herein, the precipitation polymerization approach was used to synthesize a series of ciprofloxacin molecular imprinted polymers (CIP-MIPs) by changing the solvent ratios and volume of functional monomers. Optimized CIP3-MIP and CIP6-MIP were obtained while using higher concentration ratios of ethanol, acetonitrile, and dimethyl sulfoxide. Prepared CIP-MIPs were characterized to investigate their structural interactions using the FTIR study. Surface analysis of CIP-MIPs as well as non-imprinted polymers (NIPs) was performed employing SEM and the prepared polymers exhibited porous surface having particle size 0.07 μm. EDX studies confirmed the elemental composition of CIP-MIPs. Thermal properties of CIP, CIP-MIPs and NIPs were analyzed using TGD/DTG. Moreover, CIP-MIPs were employed to remove CIP from aqueous media using well established rebinding parameters including initial CIP concentration, adsorbent dosage of CIP-MIPs, pH and agitation rate. The findings of batch binding studies illustrated that optimized CIP3-MIPs and CIP6-MIPs were able to rebind about 99.1% and 97.24%, respectively of CIP at initial CIP concentration 20 ppm, polymer dosage of 0.3 g at pH 7 and the agitation speed of 150 rpm. The imprinting factor of 1.73 and 1.699 were an indicator towards higher selectivity of CIP3-MIP and CIP6-MIP towards CIP, respectively. In addition, minimum loss of only 2.05% and 2.84% in the removal efficiency within 10 sequential cycles of adsorption–desorption process proved that CIP3-MIPs and CIP6-MIPs might be employed as the cost effective and suitable adsorbents for the removal of CIP from water bodies.

1 | Introduction

Ciprofloxacin (CIP) belongs to the fluoroquinolone class, has been effectively used to treat a broad spectrum of infections caused by a variety of bacteria, and has been listed as an important medication by the World Health Organization. Ciprofloxacin has multiple administration routes including intravenous, oral, and inhalable formulation [1]. However, the discharge of this important antibiotic molecule may cause serious water pollution when discharged into water bodies [2]. The major sources of discharge of CIP into water bodies include animal as well as human excrement [3], wastewater from hospitals, and direct release formulations development processes, during the synthesis of the active substances or even during analysis [4–6]. The amount of CIP discharged from these sources is quite high and can pose a risk for the ecosystem, which prevents the development of bacteria, may cause propagation of antibiotic-resistant species, and reduces

This is an open access article under the terms of the Creative Commons Attribution-NonCommercial License, which permits use, distribution and reproduction in any medium, provided the original work is properly cited and is not used for commercial purposes.

© 2026 The Author(s). *Polymers for Advanced Technologies* published by John Wiley & Sons Ltd.

algal diversity [6, 7]. CIP is a nondegradable and much more persistent molecule and can survive in environments for longer periods of time, spread further, and build up to larger concentrations. It is therefore much needed to develop a robust, efficient, and economical approach to deal with the removal of CIP from aqueous media. Several techniques such as adsorption, osmosis, flotation, and coagulation have been developed to deal with CIP removal [8–10]. Although these techniques are working well, these techniques are not specific towards target pollutants and face challenges of competitive adsorption phenomena, cost effectiveness, and tangible working processes. In this regard, molecularly imprinted polymers (MIPs) have been proved as outstanding adsorbents offering high specificity and selectivity for a targeted molecule [11]. In addition, MIPs find their applications in diverse fields such as environmental separation tools [12–17], in health care diagnosis [18, 19], artificial antibodies in disease detection [20], as antibody mimics [21], health surveillance and environmental monitoring [22], bio sensing [23] and in food safety and detection [24]. The MIPs present development of highly specific polymer cavities formally known as "chemical imprints" which are designed using a strongly crosslinked polymer matrix and template [25]. The process involves initially the creation of a template-functional monomer pre-polymerization complex followed by polymerization to achieve a certain spatial arrangement. The template molecule is eliminated/washed from the network and voids "chemical imprints" equivalent in size to the template are formed to rebind and eventually remove the target molecules [26, 27]. The most popular technique employed to develop MIPs involves a cross-linking agent to bind monomers and trap a template via covalent or non-covalent interactions [12] within the complex matrix. Non-covalent imprinting is the most prevalent, very simple, and affordable method for producing MIPs. This approach has numerous advantages, such as quick template binding to MIPs, facile template-monomer complex production, rapid template removal from polymers, and excellent applications to a variety of target molecules [28, 29]. However, the polymerization conditions must be carefully selected to reduce non-specific binding sites in order to enhance the formation of the labile complex of template and monomer. The current research work involves the development of ciprofloxacin molecular imprinted polymers for the adsorptive removal of CIP. Herein, a series of ciprofloxacin molecular imprinted polymers (CIP-MIPs) were synthesized by changing the ratio of solvents including ethanol, dimethyl sulfoxide (DMSO), and acetonitrile (ACN). The optimized CIP3-MIP and CIP6-MIP were characterized by FTIR, SEM, EDX, and TGA/DSC. The CIP3-MIP and CIP6-MIP were further evaluated for binding studies of CIP under well-established procedures.

2 | Materials and Methods

2.1 | Materials

CIP and Levofloxacin (LEV) were purchased from Wimits Pharmaceuticals Pvt. Ltd., 129 Sunder Industrial Estate Lahore. Acrylic acid (AA), 2,2-azobisisobutyronitrile (AIBN), and methylene bisacrylamide (MBA) were obtained from Shanghai Macklin Biochemical Co. Ltd. China. Acetic acid, acetone, methanol (MeOH), dimethyl sulfoxide (DMSO), and acetonitrile (ACN) were acquired from Sigma Aldrich Chemicals, USA.

2.2 | Equipment

The UV–Vis spectrophotometer (Agilent Cary 60) was employed to assess the concentration and absorbance of CIP solutions. Infrared spectra (IR) of the developed polymers were recorded using the FTIR Thermo Scientific Nicoleti S10, before and after the complete removal of the template molecules. The morphology and elemental analysis were conducted using a scanning electron microscope (JEOL JSM-6390LA) integrated with an energy-dispersive X-ray analyzer (EDX/EDA/EDS). The thermal properties of MIP-CIPs were characterized using a TGA Instrument, Universal Analyzer 2000 with Universal V4.7A software.

2.3 | Synthesis of Molecularly Imprinted Polymers

2.3.1 | Synthesis of CIP-MIPs

The synthesis technique, precipitation polymerization, was employed to develop molecular imprinted polymers according to ratios of solvents and functional monomer as presented in Table 1 [30, 31].

Ciprofloxacin (0.1 mmol) was initially dissolved in separate flasks containing different volumetric ratios of acetonitrile (ACN) and ethanol, acetonitrile (ACN) and dimethyl sulfoxide (DMSO), as well as ethanol and dimethyl sulfoxide (DMSO) respectively. Afterwards, the functional monomer AA, cross-linker MBA, and an initiator AIBN were added to these flasks. After 15 min of sonication, the solution was deoxygenated through nitrogen gas for 15 min. The sealed flasks containing reaction mixtures were placed in a water bath at 55°C and allowed to polymerize for 5 h. Then, the temperature of the mixtures was raised and maintained at 80°C for 2 h. The resulting polymer particles were then centrifuged at 6000 rpm for 20 min. Acetone was used to wash the polymers after filtration. The polymer particles were then dried for 6 h at 60°C in a furnace. As indicated in Table 1, the same process was used to create the subsequent MIPs and NIPs. There was no template molecule used in the creation of the NIPs.

In order to remove the template molecule, the produced MIPs were thoroughly washed by a solution of methanol and acetic acid (8:2) [32]. UV–VIS spectrophotometer was used to track the template's elimination at 277 nm. Finally, polymer microspheres were completely washed with pure acetone to ensure the removal of acetic acid, initiator, and residual monomer. After 6 h of drying in an oven, the particles were collected and yield was recorded.

3 | Batch Binding Assay (Rebinding Assay)

For rebinding assay, 100 cm^3 of 20 ppm standard solution of ciprofloxacin was added to three conical flasks (250 mL). Afterwards, 0.1 g of each of CIP1-MIP, CIP2-MIP, and CIP3-MIP were added to these flasks [33]. The conical flasks

10991581, 2026, 2, Downloaded from https://onlinelibrary.wiley.com/doi/10.1002/pat.70526 by National Institutes Of Health Malaysia, Wiley Online Library on [08/02/2026]. See the Terms and Conditions (https://onlinelibrary.wiley.com/terms-and-conditions) on Wiley Online Library for rules of use; OA articles are governed by the applicable Creative Commons License

TABLE 1 | Composition of imprinted (CIP-MIPs) and non-imprinted polymers (NIPs).

MIP	Solvents	Template (CIP)	Functional monomer (AA)	Cross linker (MBA)	Initiator (AIBN)
MIP 1	Ethanol:ACN 40:40	0.1 mmol	8 mmol	16 mmol	0.1 mmol
MIP 2			10 mmol		
MIP 3			12 mmol		
NIP1		0.0 mmol	12 mmol		
MIP 4	DMSO:ACN 20:60	0.1 mmol	8 mmol		
MIP 5			10 mmol		
MIP 6			12 mmol		
NIP2		0.0 mmol	12 mmol		
MIP 7	Ethanol:DMSO 40:40	0.1 mmol	8 mmol		
MIP 8			10 mmol		
MIP 9			12 mmol		
NIP3		0.0 mmol	12 mmol		

TABLE 2 | Adsorption parameters.

Sr. no.	Parameters	Variation in parameter	Constant parameters
1	Initial concentration	5, 10, 15, 20, 25, 30 ppm	Agitation speed 150 rpm, contact time 90 min, adsorbent dose 300 mg, pH 7
2	Polymer dosage	0.1, 0.2, 0.3, 0.4, 0.5, 0.6, 0.7 g	Agitation speed 150 rpm, contact time 90 min, pH 7, initial concentration 20 ppm
3	pH	5, 6, 7, 8, 9	Agitation speed 150 rpm contact time 90 min, adsorbent dose 300 mg, initial concentration 20 ppm
4	Contact time	30, 60, 90, 120, 150, 180, 210	Agitation speed 150 rpm, adsorbent dosage 300 mg, pH 7, initial concentration 20 ppm

containing CIP and CIP-MIPs were then agitated on an orbital shaker (Vortax Modal-OSM-747) at 150 rpm for 6 h continuously. The samples from these flasks were taken into glass vials after every 30 min time interval. All the samples were centrifuged for half an hour at 2000 rpm to obtain MIPs free filtrate. The same procedure was repeated for the batch binding of NIPs.

The binding efficiency of CIP by the CIP-MIPs and NIPs was measured by UV–VIS spectrophotometer at 278 nm λ_{max}. The binding efficiency of the samples is represented by Q in mg/g and absorbance capacity by Q_e. The extraction efficiency and absorbance capacity can be calculated by the following Equations (1) and (2):

$$\text{Binding efficiency } Q\,(\%) = C_i - C_f / C_i \times 100 \quad (1)$$

$$\text{Adsorption capacity } Q_e = \left(C_i - C_f\right) V / W \quad (2)$$

where C_i is defined as the initial concentration (mg/L) of CIP in solution, C_f is the final concentration (mg/L) of CIP, V is the volume (L) of CIP solution and W is the weight (g) of polymer (MIP/NIP).

3.1 | Adsorption Parameters

The binding efficacy was studied based on various parameters including pH, MIP dosage, CIP concentration, and contact time. Table 2 presents all the parameters. The same protocol was adopted during the study of all parameters given in the rebinding assay.

3.2 | Imprinting Factor of Optimized CIP3-MIPs and CIP6-MIPs

The strength of interactions of the MIPs with the template molecules is measured in terms of imprinting factor (IF) [34]. The value of the imprinting factor describes the specific recognition properties of a specific MIP and its NIP towards a particular template. The imprinting factor can best be described in terms of the following Equation (3):

$$\text{IF}\,(\alpha) = \frac{Q_{MIPs}}{Q_{NIP}} \quad (3)$$

where Q_{MIP} represents the adsorption capacity of MIP for CIP and Q_{NIP} represents the adsorption capacity of NIP for CIP. The

10991581, 2026, 2, Downloaded from https://onlinelibrary.wiley.com/doi/10.1002/pat.70526 by National Institutes Of Health Malaysia, Wiley Online Library on [08/02/2026]. See the Terms and Conditions (https://onlinelibrary.wiley.com/terms-and-conditions) on Wiley Online Library for rules of use; OA articles are governed by the applicable Creative Commons License

Imprinting factor (IF) of the selected/optimized CIP3-MIP and CIP6-MIP was calculated after collection of experimental data from batch binding assay.

3.3 | Repeated Use of Optimized CIP3-MIPs and CIP6-MIPs

The ciprofloxacin/template molecules adsorbed by the optimized CIP3-MIPs and CIP6-MIPs were regenerated from the polymer by washing with a mixture of methanol and acetic acid (8:2 v/v). The washing process was repeated until all template was completely removed from the polymer particles.

The stability and potential reuse of the optimized CIP-MIPs polymer were examined. Variation in rebinding properties of CIP-MIPs was recorded in ten sequential cycles of CIP adsorption–desorption. Repeating cycles of adsorption–desorption were performed at optimized conditions and further experimental data were computed.

3.4 | Selectivity Test for Optimized Ciprofloxacin Molecular Imprinted Polymers

The ability of MIPs to adsorb a specific analyte in the presence of one or more other interferes in its solution/matrix is called selectivity [35]. Any MIP has specific interactions (SI) along with the non-specific interactions (NSI). So, the selectivity of a MIP can be enhanced by making specific interactions (SI) stronger in comparison to non-specific interactions (NSI).

For the selectivity measurements, 80 mL of 20 ppm binary solution was prepared by mixing 40 mL of standard CIP solution (10 ppm) with 40 mL of standard 10 ppm LEV solution. LEV was selected as a competitive compound due to its structural resemblance with CIP. In this case, CIP is a template while LEV is a competitive template. Later on, CIP3-MIP and CIP6-MIP were treated against the above solution for the selectivity test. The ratio between templates (CIPs) and CIP-MIPs or NIPs with the solvent is called distribution ratio (K_D) and was calculated by the following Equation (4):

$$K_D = \left(C_i - C_f\right) V / C_f\, m \tag{4}$$

In this equation, C_i and C_f represent the initial and final concentration (g/mL) of interfering LEV in solution and V represents the volume of solution in ml and m represents the mass of CIP-MIP/NIP used. The ratio of the K_D of template (CIP) to the K_D of interferent (LEV) is known as the selectivity coefficient (K_{sel}) as demonstrated in Equation (5).

$$K_{sel} = \frac{K_D \text{ template (analyte)}}{K_D \text{ interferent (interferant)}} \tag{5}$$

where K_D template represents the batch binding assay of CIP-MIP/NIP for analyte CIP and K_D interferant shows batch binding assay of CIP-MIP/NIP for interferent LEV. The following equation is employed to record the selectivity coefficient (K'):

$$K' = K_{sel}\,(\text{antibiotic} - \text{MIP}) / K_{sel}\,(\text{NIP}) \tag{6}$$

Additionally, the following equation was used to measure the selectivity factor (β) for optimized CIP-MIPs.

$$\beta = \alpha_{template} / \alpha_{interferent} \tag{7}$$

In Equation (7), $\alpha_{template}$ is an imprinting factor towards analyte CIP, and $\alpha_{interferent}$ is an imprinting factor towards interferent (LEV).

In the optimum conditions in terms of pH, dosage of CIP-MIPs (CIP3-MIP and CIP6-MIP)/NIPs and contact time were maintained throughout the selectivity test. The containing solutions of template antibiotics (CIPs) and interferant antibiotics (LEV) were placed on an orbital shaker to get agitated at 150 rpm. After the optimum contact time, the flasks were removed from the orbital shaker so that their solutions could be filtered for the selectivity test of MIPs. The concentrations of the template CIP and the interferant LEV present in filtrates were then determined by UV–VIS spectrophotometric analysis at their respective λ_{max}.

4 | Results and Discussion

4.1 | Synthesis of CIP-MIPs

Preparation of molecularly imprinted polymers for ciprofloxacin (CIP-MIPs) is presented in Scheme 1. Molecular imprinting of molecules having average molar masses, low polarity, and a limited number of ionizable groups is more effective [36]. The imprinting effect is greatly affected by the size of the template [37], hence present study deals with a polar template, CIP, having an average molar mass (331.346 g/mol) and comprising two ionizable functional groups such as a carboxylic acid group (—COOH) and nitrogen of the piperazine ring. The non-covalent approach was applied for the preparation of CIP-MIPs, whereby the CIP-MIPs were synthesized using the precipitation polymerization method.

The development of the template-monomer complex was established by interactions including electrostatic, hydrophobic forces, and hydrogen bonding under porogenic solvent conditions prior to polymerization. The selection of functional monomer and absolute quantity of polymerization ingredients may assist in the development of MIPs having robust imprinting and extraction capacities. These factors have a remarkable impact on the stability of the prepared polymer and hence the efficacy of the MIPs to interact primarily with the required analyte [38]. A higher ratio of functional monomer with respect to the template may support the pre-polymerization template-monomer complex. Moreover, under porogenic solvent conditions, the interaction of CIP molecules with AA leads to the establishment of non-covalent interactions between them. The hydrogen bonding was the primary driving force for molecular recognition [39] between AA and CIP (target molecule). The carboxyl acid group (—COOH) of AA established hydrogen bonding with carboxylic acid, fluoro (attached to aromatic ring), keto, and amino (piperazine ring) groups of the CIP. Other nitrogen atoms and HC— sites of aromatic and non-aromatic rings may also play a role in interacting with functional monomer molecules and further support the fabrication of CIP-MIPs. MBA, a crosslinker, was used to preserve recognition sites and

10991581, 2026, 2, Downloaded from https://onlinelibrary.wiley.com/doi/10.1002/pat.70526 by National Institutes Of Health Malaysia, Wiley Online Library on [08/02/2026]. See the Terms and Conditions (https://onlinelibrary.wiley.com/terms-and-conditions) on Wiley Online Library for rules of use; OA articles are governed by the applicable Creative Commons License

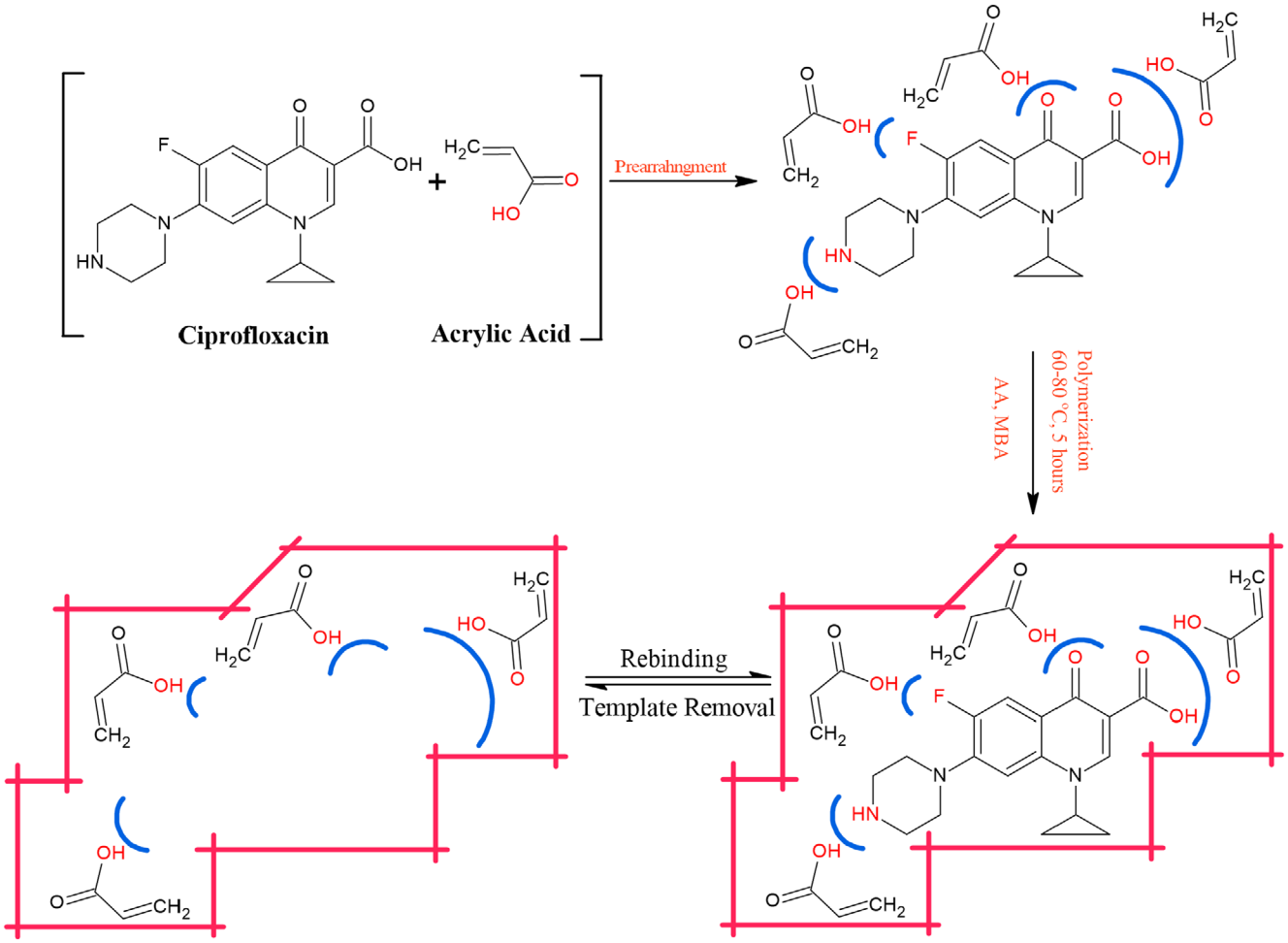

SCHEME 1 | Schematic representation for the synthesis of CIP-MIPs with CIP as a template, AA as a functional monomer, MBA as a cross-linking monomer, and AIBN as an initiator.

to maintain the backbone of CIP-MIPs. The prescribed porogenic solvent combinations, ethanol:ACN, DMSO:ACN, and ethanol:DMSO, facilitated the solubilization of the components and established interactions within CIP-MIPs, thus controlling and optimizing the distribution of imprinting cavities within the prepared CIP-MIPs. This combination of polar solvents ensured fair solubility of the CIP and played a vital role in the development of hydrogen bonds between the template (CIP) and functional monomer (AA) [40]. The appropriate combination of non-porogenic solvents had a prominent impact on the selectivity, surface area, and porosity of MIPs [40, 41]. As prepared, CIP-MIPs and NIPs were collected in powdered form having antique white and off-white colors, respectively. Finally, imprinted polymers were obtained by leaching out the CIP (template), which left the impressions corresponding to the size and structure of CIP moieties, thus can actively rebind CIP.

4.2 | FTIR Analysis

FTIR spectroscopy is a significant analysis employed to evaluate structural interactions between the functional monomers, template, and cross linker during the development of molecular imprinted polymers. Figures 1 and 2 present a comparison of FTIR spectra of MIPs, NIP-1, and ciprofloxacin before and after the removal of template. Different ratios of solvents and functional monomers provided a series of cross-linked CIP-MIPs as presented in Table 1.

Ciprofloxacin exhibited typical peaks of carboxylic acid, ketone, amine, and fluorine-substituted aromatic rings. The existence of carboxylic acid was related to peaks found at 3400 and 1725 cm^{-1} due to —OH and C═O stretching, respectively. Absorption bands at 3300 and 1650 cm^{-1} were assigned to N—H stretching and bending frequencies, respectively. Ketone (C═O) was confirmed by a stretching frequency that appeared at 1680 cm^{-1}. Another important peak at 1100 cm^{-1} was assigned to fluorine attached to the aromatic ring [42].

FTIR analysis of cross-linked CIP-MIPs was conducted before and after leaching of the ciprofloxacin. A very slight difference in the intensity and positions of absorption peaks was noticed in different CIP-MIP ratios. A peak at 1100 cm^{-1} due to aromatic fluorine was prominent in all CIP-MIPs, while this peak was found missing in NIP-1 confirming the presence of CIP in MIPs. Likewise, stretching frequencies in the FTIR spectra of un-leached CIP-MIPs, un-leached NIP-1, leached CIP-MIPs, and leached NIP-1 were also observed in the same region with a slight difference in position and intensity demonstrating that the backbone of the polymeric structure is retained.

10991581, 2026, 2, Downloaded from https://onlinelibrary.wiley.com/doi/10.1002/pat.70526 by National Institutes Of Health Malaysia, Wiley Online Library on [08/02/2026]. See the Terms and Conditions (https://onlinelibrary.wiley.com/terms-and-conditions) on Wiley Online Library for rules of use; OA articles are governed by the applicable Creative Commons License

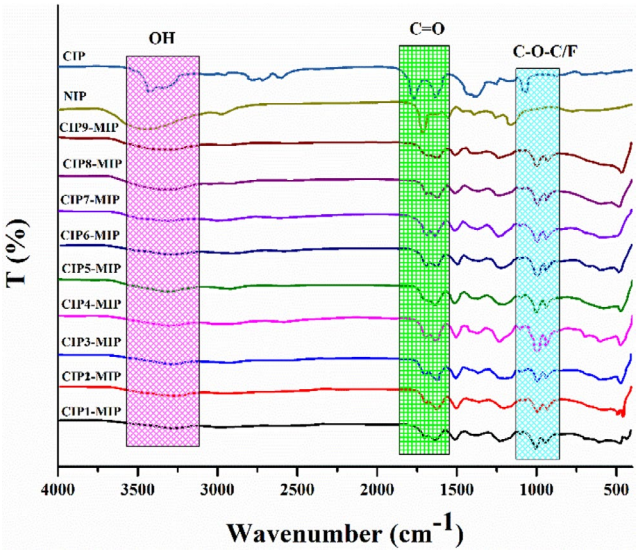

FIGURE 1 | IR spectra of unwashed CIP-MIPs1-9, NIP-1 and ciprofloxacin before washing.

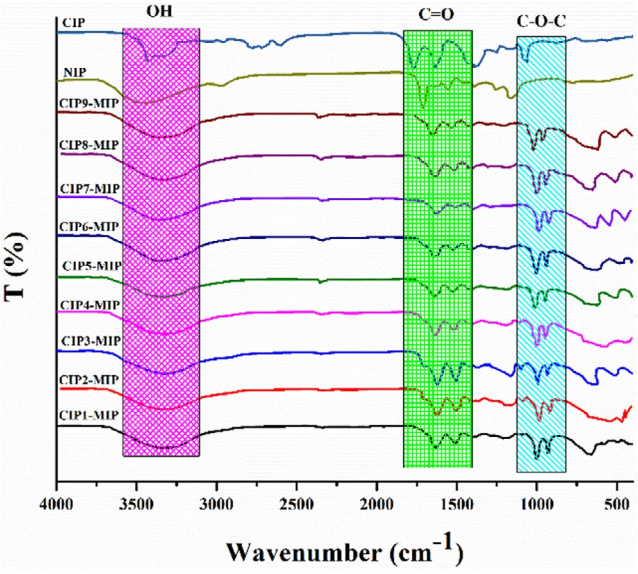

FIGURE 2 | IR spectra of CIP-MIPs1-9, NIP-1, and ciprofloxacin after washing.

A broad stretching frequency observed at 3400 cm^{-1} in the spectra of the MIPs was linked to O—H bonds from AA and CIP molecules. The existence of O—H was further complemented by bending and deformation frequencies that appeared at 1388 and 1257 cm^{-1}, respectively. The prominent peaks that appeared around 1725 cm^{-1} were assigned to carbonyl groups (C═O) present in MIPs and NIP-1. A strong peak found at 1100 cm^{-1} was attributed to aromatic fluorine stretching vibrations. The two weak stretching frequencies in the region 2988 and 2951 cm^{-1} were associated with the symmetric and asymmetric vibrations of the methylene group [35]. The existence of C═C was related to the appearance of a strong vibration frequency at 1638–1640 cm^{-1}. The outcomes of FTIR analysis illustrated the non-covalent entrapment of CIP in the MIPs [43, 44].

4.3 | SEM

SEM is a versatile tool to explore the surface properties of materials. In this study, surface properties of representative molecularly imprinted polymers CIP3-MIP and CIP6-MIP network and the respective non-imprinted polymer (NIP) were done as presented in Figure 3A–F. The SEM micrographs demonstrated that the prepared CIP-MIPs exhibited porous and spongy surface with highly uniform and well-defined cavities comprising small and monodispersed spherical particles in the range of micrometers 0.07 μm. The surface morphology showed smooth, interconnected pores, an indicative of effective washing and removal of the ciprofloxacin template. This uniform distribution of particles was attributed to non-covalent precipitation polymerization method as well as to a relatively higher proportion of acetonitrile employed during synthesis of CIP3-MIPs and CIP6-MIPs. The monodispersed MIPs offer high surface area, colloidal stability in contrast to irregular and polydispersed particles. Moreover, uniform size distribution of MIPs facilitates the efficient removal of template. Additionally, the surface roughness was moderate, ensuring an optimal surface area while maintaining mechanical stability. The cavities in CIP3-MIPs appeared to be smaller and more structured, suggesting enhanced specificity for ciprofloxacin rebinding. This uniformity in cavity distribution ensures better accessibility to the binding sites, making

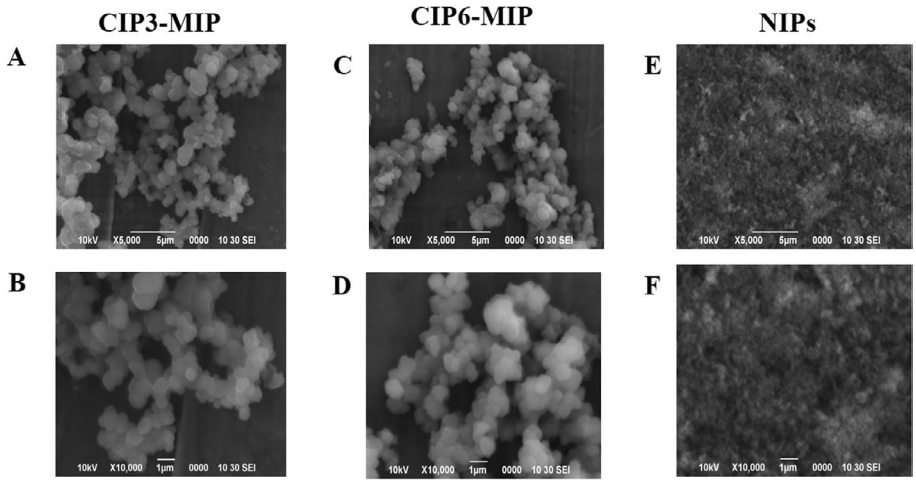

FIGURE 3 | SEM images of CP3-MIP (A, B), CP6-MIP (C, D), NIPs (E, F).

10991581, 2026, 2, Downloaded from https://onlinelibrary.wiley.com/doi/10.1002/pat.70526 by National Institutes Of Health Malaysia, Wiley Online Library on [08/02/2026]. See the Terms and Conditions (https://onlinelibrary.wiley.com/terms-and-conditions) on Wiley Online Library for rules of use; OA articles are governed by the applicable Creative Commons License

CIP3-MIPs robust for applications requiring precise molecular recognition. CIP6-MIP, on the other hand, displayed a relatively more irregular and rougher surface morphology. While the cavities were still prominent, they appeared larger and less uniformly distributed compared to CIP3-MIP. The increased roughness in CIP6-MIP suggests a higher surface area, which can enhance adsorption capacity. However, the variability in cavity sizes could affect the specificity of the polymer's rebinding properties.

The larger cavities in CIP6-MIP may also allow for binding of molecules slightly different in size to ciprofloxacin, potentially broadening its range of applications. Despite these differences, the polymer network in CIP6-MIP maintained structural integrity, making it mechanically stable and suitable for various adsorption conditions. While CIP3-MIP is superior in terms of uniformity and cavity structure, CIP6-MIP offers the advantage of a higher surface area. These morphological features suggest that CIP3-MIP might be more selective for ciprofloxacin, whereas CIP6-MIP could offer a higher adsorption capacity. Both polymers show promise, with their distinct properties suited to different application needs [45].

The SEM micrographs of NIPs are entirely different from CIP-MIPs. It is clear that NIPs are less homogeneous and relatively much smoother than CIP-MIPs. The SEM descriptions don't let it proclaim regarding the existence of high-affinity binding sites [46] within the polymer matrices, which are probably not going to be found in micrographs. However, in general, the porosity might be indicative of the existence of micro-wells inside the polymer matrices. In this context, the previous characterizations are complementary to the

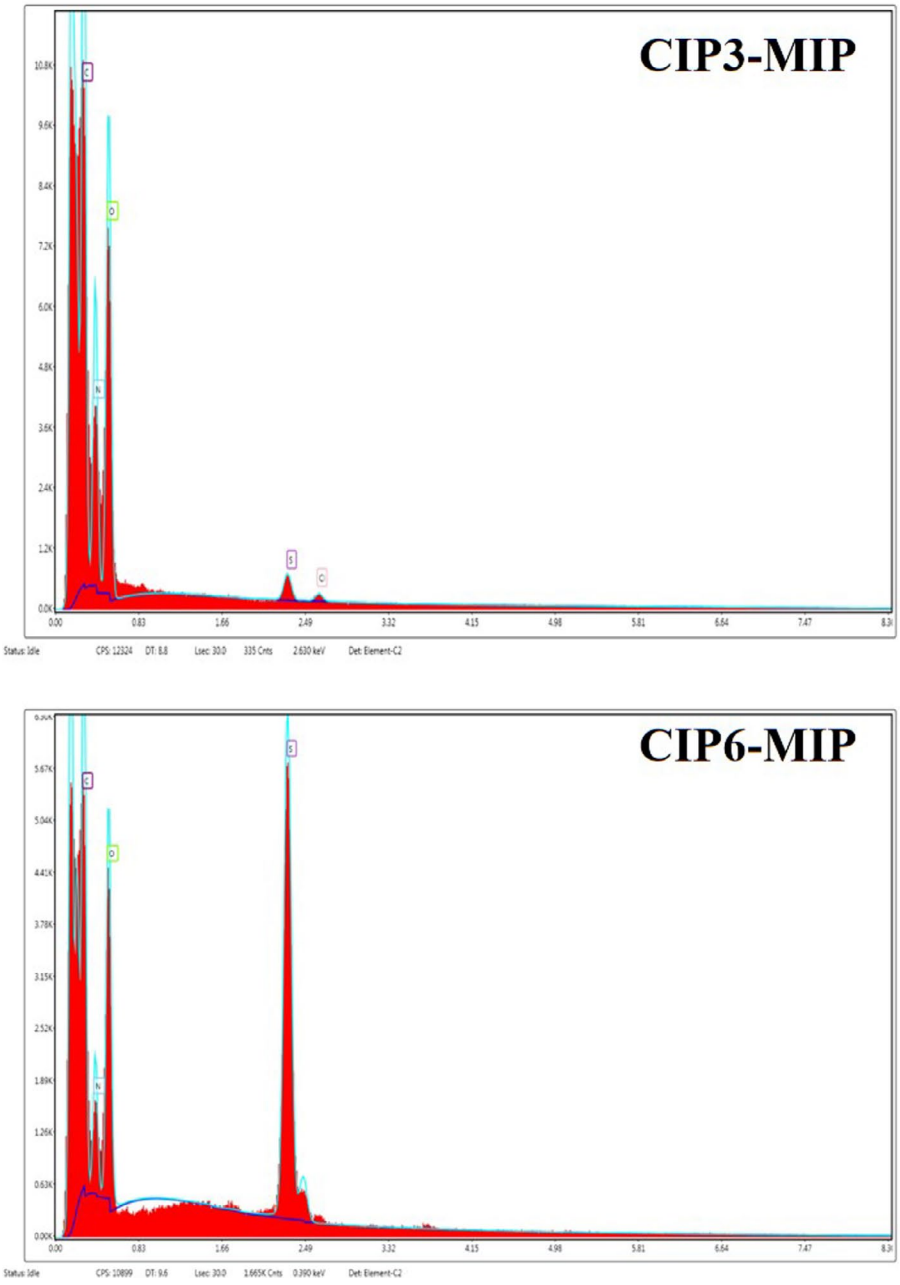

FIGURE 4 | EDX of CIP3-MIP and CIP6-MIP.

10991581, 2026, 2, Downloaded from https://onlinelibrary.wiley.com/doi/10.1002/pat.70526 by National Institutes Of Health Malaysia, Wiley Online Library on [08/02/2026]. See the Terms and Conditions (https://onlinelibrary.wiley.com/terms-and-conditions) on Wiley Online Library for rules of use; OA articles are governed by the applicable Creative Commons License

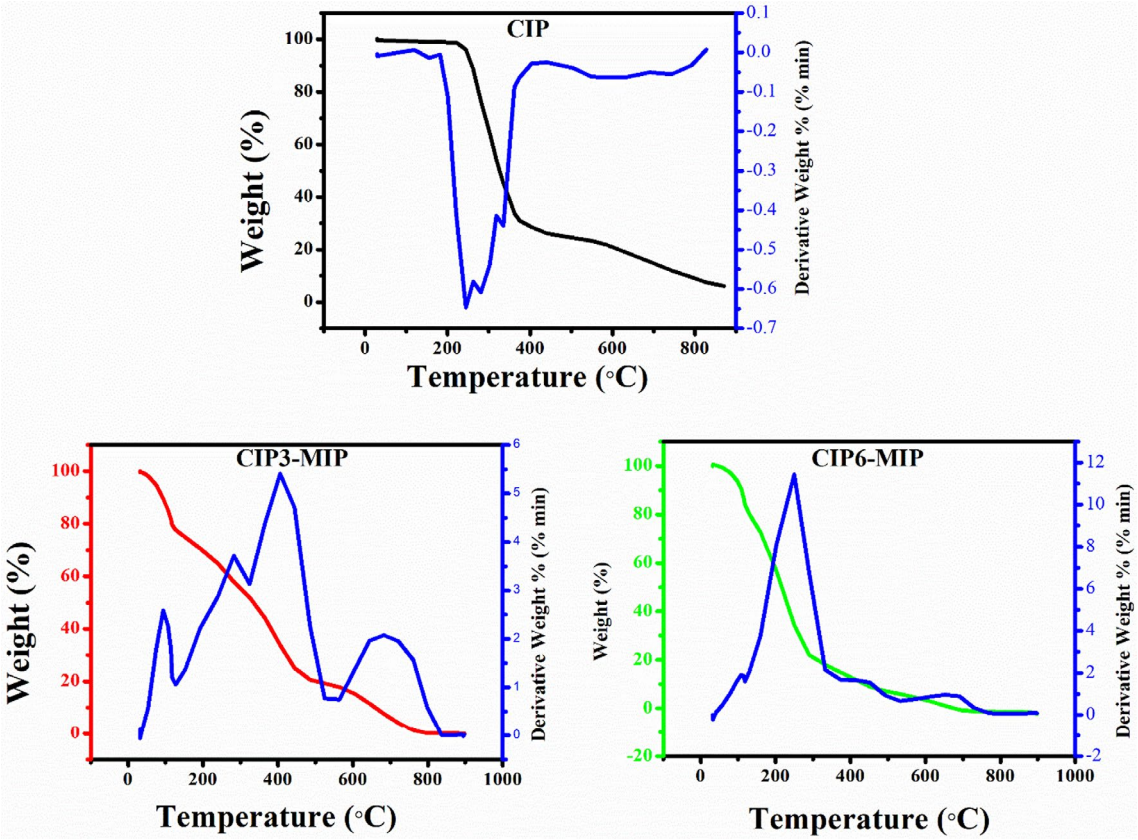

FIGURE 5 | TGA–DTA of ciprofloxacin (CIP), CIP3-MIP, and CIP6-MIP.

morphological characteristics of the MIPs and NIPs presented here [47].

4.4 | EDX

Energy-dispersive X-ray spectroscopy (EDX) was performed to find the elemental composition of developed molecularly imprinted polymers (CIP-MIPs). The peaks of carbon (C), oxygen (O), and nitrogen (N) in EDX spectra of both CIP3-MIP and CIP6-MIP confirmed the cross linking of acrylic acid (functional monomer) and methylene bisacrylamide (crosslinker) into the polymer matrix as presented in Figure 4. Imprinting of ciprofloxacin into MIP contributed to higher nitrogen content.

It was observed that in CIP3-MIPs, a higher percentage of nitrogen was observed in contrast to CIP6-MIPs, reflecting higher imprinting of ciprofloxacin and hence development of more recognition cavities. Likewise, CIP3-MIPs presented a well-defined ratio of carbon and oxygen, approving its structural integrity and improved functional monomer interaction.

On the contrary, a slightly higher content of oxygen was observed in CIP6-MIPs due to minor oxidation or more crosslinking interactions. The trace amounts of fluorine, corresponding to ciprofloxacin residues, were marginally higher in CIP3-MIP as compared to CIP6-MIP, reinforcing its superior imprinting efficiency. CIP3-MIPs elemental profile recommends that it might have enhanced binding efficacy by the dint of well-defined cavities and optimal imprinting environments compared to CIP6-MIP.

4.5 | TGA

Thermogravimetric analysis (TGA) provides critical insights into the thermal stability and decomposition patterns of molecularly imprinted polymers (MIPs). For CIP, CIP3-MIP and CIP6-MIP, TGA was performed in the range of 30°C–900°C, and results showed distinct thermal profiles that reflect the structural integrity and cross-linking efficiency of the synthesized polymers, as presented in Figure 5. The thermogram of ciprofloxacin demonstrated that it is stable up to 50°C. After 50°C, the onset of decomposition of CIP started and completed at 750°C with two stages. The initial weight loss of 8% at 130°C was related to the loss of acetylene molecule, and the second weight loss was related to decomposition between 315°C and 382°C [46]. CIP3-MIP demonstrated superior thermal stability compared to CIP6-MIP. Figure 5 showed two stages of weight loss for CIP3-MIP and CIP6-MIP. The initial weight loss (< 5%) occurred around 50°C–100°C, attributed to the evaporation of residual solvents or moisture (free and bound) trapped in the polymer matrix.

Moreover, both CIP3-MIP and CIP6-MIP exhibited significant weight loss (90%) between 200°C and 400°C, which corresponds to the degradation of the polymer backbone. However, CIP3-MIP had a slightly higher decomposition onset temperature (~260°C) compared to CIP6-MIP (240°C), indicating better cross-linking density.

Likewise, DTA curves exhibited two endothermic peaks which strongly endorsed the phenomena of degradation that occurred in the polymer. The first endothermic curve revealed the loss of

10991581, 2026, 2, Downloaded from https://onlinelibrary.wiley.com/doi/10.1002/pat.70526 by National Institutes Of Health Malaysia, Wiley Online Library on [08/02/2026]. See the Terms and Conditions (https://onlinelibrary.wiley.com/terms-and-conditions) on Wiley Online Library for rules of use; OA articles are governed by the applicable Creative Commons License

solvent and is owing to the second peak demonstrated, showing the degradation of CIP-MIPs backbone. However, the DTA of CIP3-MIPs was sharper and occurred at a higher temperature than CIP6-MIPs, suggesting that the CIP3-MIPs network was more robust. Beyond 400°C, weight loss slowed significantly, representing the breakdown of the residual carbon framework. CIP3-MIPs retained a higher percentage of mass at 600°C (~35%) compared to CIP6-MIP (~30%), confirming its enhanced thermal stability. The thermal resistance of CIP3-MIPs can be linked to its optimized cavity structure and efficient interaction between the cross-linking agent methylene bisacrylamide (MBA) and the functional monomer (acrylic acid). CIP6-MIPs, while slightly less thermally stable, exhibited similar degradation patterns but with slightly lower residual mass, suggesting minor structural weaknesses or less uniform cavity formation. These results validate CIP3-MIP as a superior polymer in terms of thermal resilience, likely enhancing its performance in practical applications, such as drug release or adsorption studies, due to its stable molecular imprinting and robust polymer matrix [47].

5 | Batch Binding Assay for CIP-MIPs

Out of the nine CIP-MIPs (CIP1-MIP, CIP2-MIP, CIP3-MIP, CIP4-MIP, CIP5-MIP, CIP6-MIP, CIP7-MIP, CIP8-MIP, and CIP9-MIP), the highest removal efficiency was shown by CIP3-MIP and CIP6-MIP. These MIPs were synthesized under optimized ratios of template, functional monomer, and cross-linker viz. 0.1:12:16 for CIP3-MIPs and 0.1:12:16 for CIP6-MIPs, respectively. Due to the absence of recognition sites in NIP-1, NIP-2, and NIP3 particles, they exhibited the least binding efficiency. Figure 6 precisely portrays the binding efficiencies of developed CIP-MIPs and NIPs. Due to the highest removal efficacy of CIP3-MIP and CIP6-MIP, these two imprinted polymers were selected for further investigation of batching binding under well-established parameters.

5.1 | Effect of the Contact Time

Contact time of adsorbent and adsorbate has significant impact on batch binding assay. The effect of contact time on the adsorption of CIP by CIP-MIPs has been presented in Figure 7A. It is evident from the results that maximum liquid phase [48] extraction of ciprofloxacin by the CIP3-MIPs as well as CIP6-MIPs was achieved after 150 min. As observed in case of parameters, rate of adsorption was high in the beginning followed by a dynamic equilibrium and further becomes constant or decreases. A similar trend was observed in the case of contact time. The removal efficiency (% R) of CIP-MIPs increased with the increase in contact time. This trend may be associated with the fact that in the beginning, the CIP molecules move rapidly towards the MIPs, as the binding sites present in MIPs are completely deficient of the template molecules leading towards a higher removal efficiency in the beginning. With the passage of time, the removal efficiency of CIP-MIPs becomes almost constant. A state of dynamic equilibrium in the MIPs cavities was

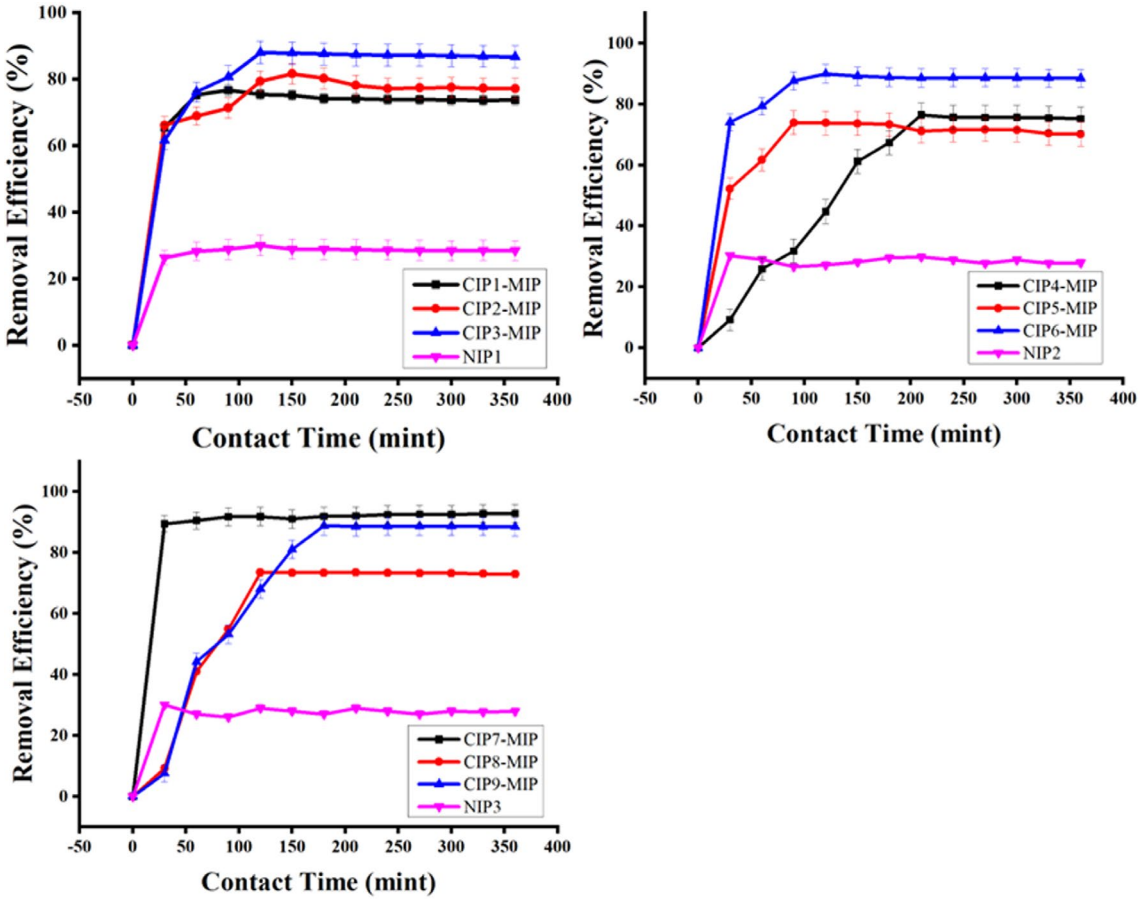

FIGURE 6 | Effect of CIP-MIPs (CIP1-MIP to CIP9-MIP) and NIPs (NIP1 to NIP3) on percentage removal efficiency of CIP under optimized conditions (initial concentration: 20 ppm, dosage: 0.3 g, pH: 7, agitation: 150 rpm). Error bars indicate ±SD = 0.73 ($n = 3$).

10991581, 2026, 2, Downloaded from https://onlinelibrary.wiley.com/doi/10.1002/pat.70526 by National Institutes Of Health Malaysia, Wiley Online Library on [08/02/2026]. See the Terms and Conditions (https://onlinelibrary.wiley.com/terms-and-conditions) on Wiley Online Library for rules of use; OA articles are governed by the applicable Creative Commons License

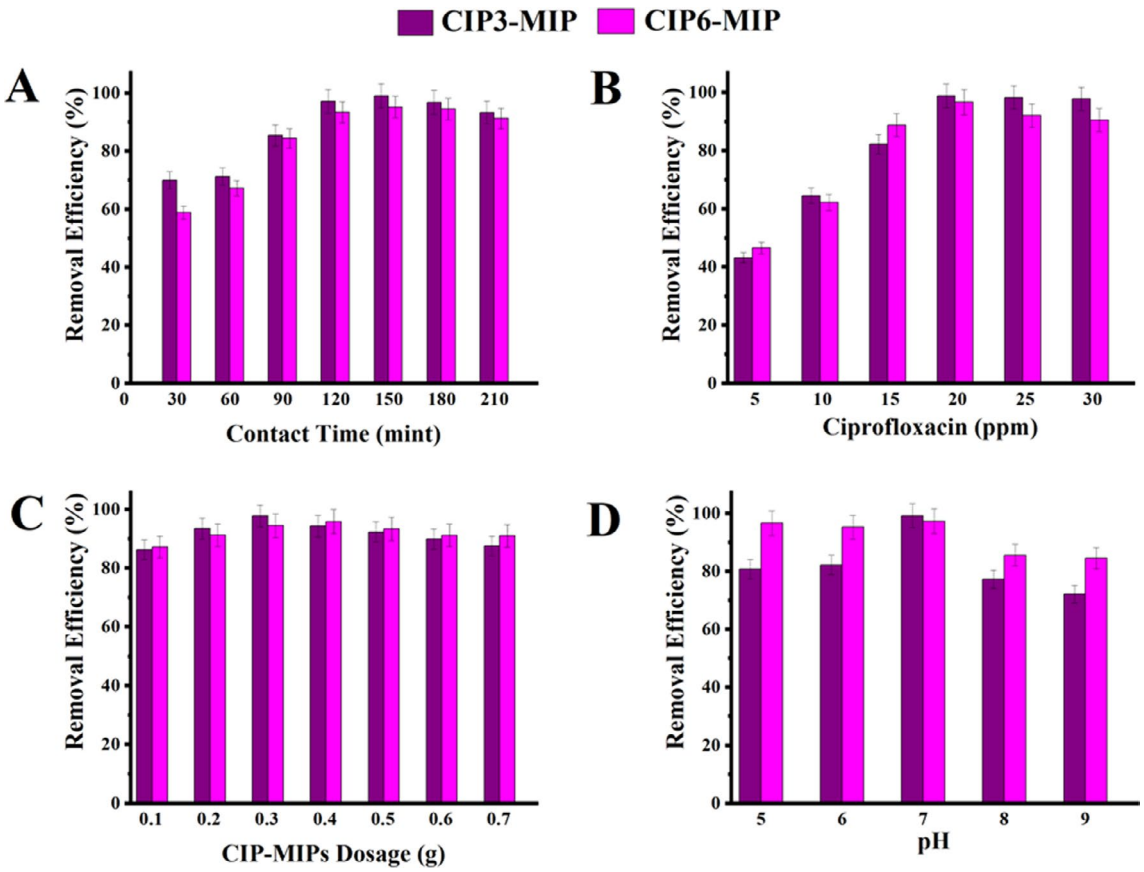

FIGURE 7 | Effect of contact time (A), CIP concentration (B), MIP dosage (C), and pH (D) on percentage removal of CIP using CIP3-MIP and CIP6-MIP. Conditions: Agitation 150 rpm, temperature 25°C. Error bars indicate ±SD = 0.79 ($n = 3$).

TABLE 3 | Study of process parameters on the adsorption/sorption by selected CIP-MIPs.

Molecularly imprinted polymer	Process parameters				
	Agitation/ contact time	Concentration	Dosage	pH	IF (α) IF(α) = Q(CIP − MIP)/ Q_{NIP}
CIP3-MIP	150 min	20 ppm	0.2 g	7	
	$Q = 98.99$	$Q = 98.81$	$Q = 97.76$	$Q = 99.1$	IF (α) = 1.73
	$Q_e = 19.79$	$Q_e = 19.76$	$Q_e = 9.78$	$Q_e = 19.82$	
CIP6-MIP	150 min	20 ppm	0.3 g	7	
	$Q = 95.15$	$Q = 96.62$	$Q = 95.78$	$Q = 97.2$	IF (α) = 1.699
	$Q_e = 19.03$	$Q_e = 19.32$	$Q_e = 6.38$	$Q_e = 19.44$	

Note: Values represent Mean ± SD CIP3-MIP(Q) = 0.62, Mean ± SD CIP6-MIP(Q) = 0.90, ($n = 4$).

established between the amount of CIP being adsorbed by the MIPs and that desorbed from the polymer molecules. The binding cavities of the MIPs are almost saturated with the antibiotic molecules and hence do not permit further adsorption to take place [49, 50].

5.2 | Effect of CIP Concentration on Uptake Behavior by CIP3-MIP and CIP6-MIP

The concentration of template (CIP) solution has a noticeable impact on the removal efficiency of the CIP-MIPs. It was observed that the removal efficiency of selected MIPs (CIP3-MIP, CIP6-MIP) increased with the increasing concentration of CIP solution in the beginning up to a certain concentration range as shown in Figure 7B. It is due to the fact that the solutions with higher concentration of CIP have higher number of target molecules which in turn surrounded the active binding sites of the polymer effectively, leading towards a better and efficient adsorption. This trend may also be attributed to the fact that when concentration of template molecules is higher, then responsible driving forces for mass transfer will be relatively high. For CIP3-MIP and CIP6-MIP, the maximum % removal efficiency was observed at 98.81% and 96.62%, respectively

10991581, 2026, 2, Downloaded from https://onlinelibrary.wiley.com/doi/10.1002/pat.70526 by National Institutes Of Health Malaysia, Wiley Online Library on [08/02/2026]. See the Terms and Conditions (https://onlinelibrary.wiley.com/terms-and-conditions) on Wiley Online Library for rules of use; OA articles are governed by the applicable Creative Commons License

with the CIP solution concentration of 20 ppm. Beyond this level of concentration, the % removal efficiency remains almost constant. It is due to the fact that all the binding sites have already been occupied by the target CIP molecules. So, no space was available for the newly incoming molecules of CIP in the polymer cavities [51, 52].

5.3 | Effect of CIP3-MIP and CIP6-MIP Dosage on Uptake Behavior of CIP

This initial increase in percentage removal with increased polymer dosage was related to the availability of all binding sites where the target CIP molecules got adsorbed and hence the adsorption of the CIP-MIPs increased. Experiments illustrated that CIP3-MIP exhibited 97.76% removal efficiency at a polymer dosage of 0.2 g and CIP6-MIP presented the highest removal efficiency of 95.78% at 0.3 g of polymer dosage. It was established that adsorbent dosages of 0.2 g and 0.3 g are the optimum dosages of the CIP3-MIPs and CIP6-MIPs respectively under optimized conditions of contact time and solution concentrations [50, 51]. Moreover, the decline in percentage removal efficiency after the optimized dosage was related to the phenomenon of accumulation of MIP particles got in the form of heap which reduced the number of active sites availability and hence the removal efficiency of CIP-MIPs decreased [49, 50].

TABLE 4 | Effect of reused times on the % R of optimized CIP3-MIP and CIP6-MIP.

Adsorption–desorption cycle	% R (Q) for CIP	
	CIP3-MIP (%)	CIP6-MIP (%)
Cycle-1	99.10	97.24
Cycle-2	98.85	97.12
Cycle-3	98.59	97.11
Cycle-4	98.42	96.88
Cycle-5	98.21	96.61
Cycle-6	97.71	96.21
Cycle-7	97.50	96.01
Cycle-8	97.42	95.31
Cycle-9	97.26	95.06
Cycle-10	97.05	94.40
Overall loss after 10 cycles	2.05	2.84

Note: Values represent Mean ± SD CIP3-MIP = 0.72, ± SD CIP6-MIP = 0.99, $n = 10$.

5.4 | Effect of CIP Solution pH on Uptake Behavior by CIP3-MIP

Batch binding study of CIP over CIP3-MIP and CIP6-MIP was investigated over a pH 5 to pH 9. The highest percentage removal efficiency of ciprofloxacin was observed at pH 7; beyond this pH, the majority of CIP molecules adopted zwitter ionic configuration. At pH 1, 99.9% of the samples have the charge positive form QH^{2+}. However, under neutral conditions, both functional groups of CIP molecules were active and available for bonding, and the binding sites in the MIP cavities offered chemical speciation. Under acidic and basic conditions, modification in the cavity or CIP molecules configurations led to improper fit towards the binding sites, which affected the removal efficiency and adsorption capacity.

6 | Imprinting Factor of Optimized CIP3-MIPs and CIP6-MIPs

Imprinting factors (α) are significant indicators towards definite recognition characteristics of CIP-MIPs for CIP template with respect to its NIP. IF is related to the ratio of the template (CIP) molecules entrapped in CIP-MIPs cavities versus the template (CIP) attached to the NIP. Higher values of IF stand for stronger interactions of template molecules with MIPs leading towards higher adsorption capacities (Q_e). Table 3 shows IF (α) value for the CIP3-MIP and CIP6-MIP. CIP3-MIP and CIP6-MIPs exhibited higher IF value (α) of 1.73 and 1.699 presenting enhanced degrees of imprinting in them. These noteworthy IF values for CIP3-MIPand CIP6-MIP also related to the application of appropriate polar solvent systems. Hence, polar solvents with reasonable combinations are good porogenic solvent compositions for synthesis of CIP-MIPs [37].

7 | Repeated Use of Optimized CIP-MIPs

The ability of recognition is one of the outstanding features of MIPs. This ability enables MIPs to adsorb specific molecules repeatedly and restore their recognition property and maintain their adsorption capacity with minimal change [13]. To validate the ability of recognition, 10 cycles

TABLE 5 | The distribution ratio, selectivity coefficient, relative selectivity coefficient, and selectivity factor for optimized CIP3-MIP, CIP6-MIP, and NIPs.

Imprinted polymer	Target	K_D (MIP)	K_D (NIP)	K^{sel} (MIP)	K^{sel} (NIP)	K''	B
CIP3-MIP	Template (CIP)	18.35	0.222	3.972	1.275	3.115	3.17
	Interferent (LEV)	4.619	0.174				
CIP6-MIP	Template (CIP)	5.87	0.222	3.891	1.313	2.963	2.81
	Interferent (LEV)	1.508	0.169				

10991581, 2026, 2, Downloaded from https://onlinelibrary.wiley.com/doi/10.1002/pat.70526 by National Institutes Of Health Malaysia, Wiley Online Library on [08/02/2026]. See the Terms and Conditions (https://onlinelibrary.wiley.com/terms-and-conditions) on Wiley Online Library for rules of use; OA articles are governed by the applicable Creative Commons License

of adsorption–desorption phenomenon were repeated under optimized conditions of initial concentration of CIP, dosage of CIP-MIPs, agitation time, and pH. Experimental data illustrated that CIP-MIPs maintained enough stability during the adsorption–desorption cycles without a remarkable variation in the removal efficiency. Table 4 demonstrates that approximately 2.05% difference in CIP rebinding assay was observed in case of CIP3-MIPs and 2.84% in case of CIP6-MIPs after 10 cycles. This negligible loss is evidence of the ability for recognition of MIPs.

8 | Selectivity Test for Optimized CIP-MIPs

To investigate the sensing property of CIP-MIPs, a selectivity test was performed. For this test, Levofloxacin (LEV) was taken as a suitable interfering and competitive molecule for CIP due to structural resemblance between these two drugs. Both drugs belong to the fluoroquinolone class and exhibit similar physical and chemical characteristics. The experiments were performed on a UV–VIS spectrophotometer, and the obtained data was used to calculate distribution ratios (K_D), selectivity coefficients (K_{sel}), relative selectivity coefficients (k'), and selectivity factors (β) as presented in Table 5. It was found that mixing appropriate ratios of solvents and cross-linker during reaction leads to the development of many high-affinity sites, which may affect template distribution ratios in MIPs. Herein, the distribution ratio is a measure of comparison of the adsorbed amount of the template and the interferent with having the same initial concentration.

The outcomes of the study illustrated that distribution ratios of CIP in CIP3-MIP and CIP6-MIP were prominently greater as compared to the distribution ratios of its competitor (LEV). The remarkable selectivity coefficient values demonstrated that CIP3-MIP and CIP6-MIP are highly specific for CIP removal, and the imprinting approach was accurately operative. The molecular recognition process may well be understood by the selectivity tests of the CIP3-MIP and CIP6-MIP. Although CIP and LEV are structurally analogous to each other, there are a few dissimilarities which make CIP a more fit template. CIP exhibits relatively smaller spatial diameter as compared to LEV. The core structure of both antibiotic drugs is the same, having a fluorine atom at position 6, a carboxylic acid (-COOH) group at position 3, and a nitrogen-containing group at position 7. CIP is more flexible due to the presence of piperazine rings and tends to adopt different conformations, while levofloxacin is chiral and more rigid. Moreover, CIP is less hydrophilic as compared to LEV. The structural analysis supported that structural compatibility of CIP might present promising interactions with the active binding sites of CIP-MIPs and paved a way for facile entrapment into the cavities as compared to LEV. The performance of CIP-MIPs depicted that they have more selectivity for CIP (template). The distribution ratios of CIP were also recorded higher due to the reason that CIP-MIPs may recognize and coordinate the CIP molecules by specific active binding sites that have been preserved as a memory [13]. Template (CIP) molecules may easily interact with the comparable cavities present in CIP-MIPs, while an interferent (LEV) presents poor interactions attributed to nonspecific interactions. Additionally, template (CIP) molecules and interferent (LEV) exhibited more associations in the CIP-MIPs as compared to NIPs because NIPs lack binding sites. So, adsorption of CIP by CIP-MIPs is one of the best separation techniques [53] to make castoff water antibiotics free.

9 | Conclusion

In the present research, molecular imprinted polymers for ciprofloxacin (CIP-MIPs) were successfully synthesized by precipitation polymerization method using several porogenic solvent mixtures (ethanol, acetonitrile and dimethyl sulfoxide). The developed CIP-MIPs were stabilized by non-covalent forces and a new experimental series of CIP-MIPs with CIP as the template and MBA cross linker were developed by changing the molar ratios of solvents and functional monomer. The study illustrated that the two selected CIP-MIPs were prepared at the same optimized ratios of 0.1:12:16 for template, functional monomer and cross linker but with different porogenic solvents. Both CIP3-MIP and CIP6-MIP exhibited percentage removal of about 99.1% and 97.24% respectively at optimum conditions (contact time 150 min, polymer dosage 0.3 g, concentration 20 ppm, and pH 7). The most prominent finding of the present study is that CIP-MIPs are highly selective having greater than 95% of removal efficacy and can be used efficiently for the decontamination [13] of aqueous media.

The successful preparation and removal of CIP from MIPs was confirmed by FTIR. SEM results demonstrated spherical particles having an average diameter of 0.07 μm. Moreover, thermal properties were ascertained by TGA. These findings and results demonstrated that CIP3-MIPs and CIP6-MIPs were optimized polymers having outstanding performance to remove CIP. Furthermore, this approach highlighted the benefits of using and recycling MIPs with comparable rebinding capacity several times in aqueous bodies and for environmental monitoring [13].

Conflicts of Interest

The authors declare no conflicts of interest.

Data Availability Statement

The data that support the findings of this study are available from the corresponding author upon reasonable request.

References

1. V. K. Panthi, K. E. Fairfull-Smith, and N. Islam, "Ciprofloxacin-Loaded Inhalable Formulations Against Lower Respiratory Tract Infections: Challenges, Recent Advances, and Future Perspectives," *Pharmaceutics* 16, no. 5 (2024): 648, https://doi.org/10.3390/pharmaceutics16050648.

2. M. F. Moradali, S. Ghods, and B. H. Rehm, "*Pseudomonas Aeruginosa* Lifestyle: A Paradigm for Adaptation, Survival, and Persistence," *Frontiers in Cellular and Infection Microbiology* 7 (2017): 39, https://doi.org/10.3389/fcimb.2017.00039.

3. T. Trouchon and S. Lefebvre, "A Review of Enrofloxacin for Veterinary Use," *Open Journal of Veterinary Medicine* 6, no. 2 (2016): 40–58, https://doi.org/10.4236/ojvm.2016.62006.

4. P. A. Segura, M. François, C. Gagnon, and S. Sauvé, "Review of the Occurrence of Anti-Infectives in Contaminated Wastewaters and

10991581, 2026, 2, Downloaded from https://onlinelibrary.wiley.com/doi/10.1002/pat.70526 by National Institutes Of Health Malaysia, Wiley Online Library on [08/02/2026]. See the Terms and Conditions (https://onlinelibrary.wiley.com/terms-and-conditions) on Wiley Online Library for rules of use; OA articles are governed by the applicable Creative Commons License

Natural and Drinking Waters," *Environmental Health Perspectives* 117, no. 5 (2009): 675–684, https://doi.org/10.1289/ehp.11776.

5. C. Rodrigues-Silva, M. G. Maniero, M. S. Peres, and J. R. Guimarães, "Ocorrência e Degradação de Quinolonas por Processos Oxidativos Avançados," *Química Nova* 37 (2014): 868–885, https://doi.org/10.5935/0100-4042.20140123.

6. C. Girardi, J. Greve, M. Lamshöft, et al., "Biodegradation of Ciprofloxacin in Water and Soil and Its Effects on the Microbial Communities," *Journal of Hazardous Materials* 198 (2011): 22–30, https://doi.org/10.1016/j.jhazmat.2011.10.004.

7. V. Diniz, G. Rath, S. Rath, C. Rodrigues-Silva, J. R. Guimarães, and D. G. Cunha, "Long-Term Ecotoxicological Effects of Ciprofloxacin in Combination With Caffeine on the Microalga *Raphidocelis subcapitata*," *Toxicology Reports* 8 (2021): 429–435, https://doi.org/10.1016/j.toxrep.2021.02.016.

8. C. A. Igwegbe, S. N. Oba, C. O. Aniagor, A. G. Adeniyi, and J. O. Ighalo, "Adsorption of Ciprofloxacin From Water: A Comprehensive Review," *Journal of Industrial and Engineering Chemistry* 93 (2021): 57–77, https://doi.org/10.1016/j.jiec.2020.09.016.

9. S. W. Alberti, F. B. Scheufele, V. Steffen, and E. A. da Silva, "Adsorption of Ciprofloxacin From Aqueous Media by Activated Carbon: A Review," *Water Conservation Science and Engineering* 9, no. 1 (2024): 26, https://doi.org/10.1007/s41101-024-00185-3.

10. P. Khan, R. Saha, and G. Halder, "Towards Sorptive Eradication of Pharmaceutical Micro-Pollutant Ciprofloxacin From Aquatic Environment: A Comprehensive Review," *Science of the Total Environment* 919 (2024): 170723, https://doi.org/10.1016/j.scitotenv.2024.170723.

11. X. Song, J. Li, J. Wang, and L. Chen, "Quercetin Molecularly Imprinted Polymers: Preparation, Recognition Characteristics and Properties as Sorbent for Solid-Phase Extraction," *Talanta* 80, no. 2 (2009): 694–702, https://doi.org/10.1016/j.talanta.2009.07.059.

12. D. A. Gkika, A. K. Tolkou, D. A. Lambropoulou, et al., "Application of Molecularly Imprinted Polymers (MIPs) as Environmental Separation Tools," *RSC Applied Polymers* 2, no. 2 (2024): 127–148, https://doi.org/10.1039/D3LP00202F.

13. A.-M. Gavrilă, M. Ioniță, and G. Toader, "Recent Advances in Molecularly Imprinted Polymers and Emerging Polymeric Technologies for Hazardous Compounds," *Polymers* 17 (2025): 1092, https://doi.org/10.3390/polym17081092.

14. G. Heidari, F. H. Afruzi, and E. N. Zare, "Molecularly Imprinted Magnetic Nanocomposite Based on Carboxymethyl Dextrin for Removal of Ciprofloxacin Antibiotic From Contaminated Water," *Nanomaterials* 13 (2023): 489, https://doi.org/10.3390/nano13030489.

15. S. Bathula, S. Thottathil, and Y. M. Puttaiahgowda, "MOFs and MOF-Based Composites for the Adsorptive Removal of Ciprofloxacin," *Macromolecular Materials and Engineering* 310 (2025): 2400238, https://doi.org/10.1002/mame.202400238.

16. S. M. Mahgoub, H. A. Rudayni, A. A. Allam, et al., "Green Removal and Waste Valorization of Ciprofloxacin From Water Using Zinc–Iron LDH–Chia Seed Biocomposites: Integrated Adsorption, Computational Modeling, and Electrochemical Conversion," *RSC Advances* 15 (2025): 37705–37726, https://doi.org/10.1039/D5RA06018D.

17. F. I. Rabu, S. F. F. S. Yaacob, I. O. Saheed, M. A. K. M. Hanafiah, A. F. A. Latip, and F. B. M. Suah, "Harnessing Sporopollenin-Based Polymer Membranes: An Exploratory Study on Ciprofloxacin Removal," *Pure and Applied Chemistry* 97 (2025): 945–955, https://doi.org/10.1515/pac-2024-0393.

18. A. G. Ayankojo, J. Reut, and V. Syritski, "Electrochemically Synthesized MIP Sensors: Applications in Healthcare Diagnostics," *Biosensors* 14, no. 2 (2024): 71, https://doi.org/10.3390/bios14020071.

19. Y. Li, C. Guan, C. Liu, Z. Li, and G. Han, "Disease Diagnosis and Application Analysis of Molecularly Imprinted Polymers (MIPs) in Saliva Detection," *Talanta* 269 (2024): 125394, https://doi.org/10.1016/j.talanta.2023.125394.

20. V. Milanković, T. Tasić, I. A. Pašti, and T. Lazarević-Pašti, "MIP-Based Optical Sensors: Exploring Principles and Applications as Artificial Antibodies in Disease Detection and Monitoring," in *Molecularly Imprinted Polymers: Path to Artificial Antibodies* (Springer, 2024), 273–297, https://doi.org/10.1007/978-3-031-60095-6_14.

21. M. Gamal, M. S. Imam, A. S. Albugami, et al., "Current Advances in the Implementation of Magnetic Molecularly Imprinted Polymers Tailored for Enrichment of Target Analytes in Different Environmental Samples: An Overview From a Comprehensive Perspective," *Trends in Environmental Analytical Chemistry* 43 (2024): e00236, https://doi.org/10.1016/j.teac.2024.e00236.

22. M. S. Sengar, P. Kumari, N. Sengar, and S. K. Singh, "Molecularly Imprinted Polymer Technology for the Advancement of Its Health Surveillances and Environmental Monitoring," *ACS Applied Polymer Materials* 6, no. 2 (2024): 1086–1105, https://doi.org/10.1021/acsapm.3c01851.

23. Y. Saylan, S. Kılıç, and A. Denizli, "Biosensing Applications of Molecularly Imprinted-Polymer-Based Nanomaterials," *PRO* 12, no. 1 (2024): 177, https://doi.org/10.3390/pr12010177.

24. L. Geng, J. Huang, M. Fang, et al., "Recent Progress of the Research of Metal-Organic Frameworks-Molecularly Imprinted Polymers (MOFs-MIPs) in Food Safety Detection Field," *Food Chemistry* 458 (2024): 140330, https://doi.org/10.1016/j.foodchem.2024.140330.

25. Y. Liu, L. Wang, H. Li, et al., "Rigorous Recognition Mode Analysis of Molecularly Imprinted Polymers—Rational Design, Challenges, and Opportunities," *Progress in Polymer Science* 150 (2024): 101790, https://doi.org/10.1016/j.progpolymsci.2024.101790.

26. T. Sajini and B. Mathew, "A Brief Overview of Molecularly Imprinted Polymers: Highlighting Computational Design, Nano and Photo-Responsive Imprinting," *Talanta Open* 4 (2021): 100072, https://doi.org/10.1016/j.talo.2021.100072.

27. S. Bahrani, R. Aslani, S. A. Hashemi, S. M. Mousavi, and M. Ghaedi, "Introduction to Molecularly Imprinted Polymer," in *Interface Science and Technology*, vol. 33 (Elsevier, 2021), 511–556, https://doi.org/10.1016/B978-0-12-824574-9.00017-2.

28. A. Öpik, A. Menaker, J. Reut, and V. Syritski, "Molecularly Imprinted Polymers: A New Approach to the Preparation of Functional Materials," *Proceedings of the Estonian Academy of Sciences* 58, no. 1 (2009): 3–11, https://doi.org/10.3176/proc.2009.1.01.

29. A. Lusina, T. Nazim, and M. Cegłowski, "Synthesis and Characterization of MIPs," in *Molecularly Imprinted Polymers: Path to Artificial Antibodies* (Springer, 2024), 29–67, https://doi.org/10.1007/978-3-031-50515-4_2.

30. S. A. Bhawani, T. S. Sen, and M. N. M. Ibrahim, "Synthesis of Molecular Imprinting Polymers for Extraction of Gallic Acid From Urine," *Chemistry Central Journal* 12 (2018): 7, https://doi.org/10.1186/s13065-018-0372-6.

31. A. L. Joke Chow and S. A. Bhawani, "Synthesis and Characterization of Molecular Imprinting Polymer Microspheres of Cinnamic Acid: Extraction of Cinnamic Acid From Spiked Blood Plasma," *International Journal of Polymeric Science* 2016, no. 1 (2016): 2418915, https://doi.org/10.1155/2016/2418915.

32. D. Singh and S. Mishra, "Synthesis and Characterization of Hg(II)-Ion-Imprinted Polymer: Kinetic and Isotherm Studies," *Desalination* 257, no. 1–3 (2010): 177–183, https://doi.org/10.1016/j.desal.2010.02.032.

33. R. J. Ansell, "Characterization of the Binding Properties of Molecularly Imprinted Polymers," in *Molecularly Imprinted Polymers in Biotechnology. Advances in Biochemical Engineering/Biotechnology*, vol. 150, ed. B. Mattiasson and L. Ye (Springer International Publishing, 2015), 51–93, https://doi.org/10.1007/10_2015_316.

10991581, 2026, 2, Downloaded from https://onlinelibrary.wiley.com/doi/10.1002/pat.70526 by National Institutes Of Health Malaysia, Wiley Online Library on [08/02/2026]. See the Terms and Conditions (https://onlinelibrary.wiley.com/terms-and-conditions) on Wiley Online Library for rules of use; OA articles are governed by the applicable Creative Commons License

34. A. N. Hasanah, N. Safitri, A. Zulfa, N. Neli, and D. Rahayu, "Factors Affecting Preparation of Molecularly Imprinted Polymer and Methods on Finding Template–Monomer Interaction as the Key of Selective Properties of the Materials," *Molecules* 26, no. 18 (2021): 5612, https://doi.org/10.3390/molecules26185612.

35. S. R. Shafqat, S. A. Bhawani, S. Bakhtiar, M. N. M. Ibrahim, and S. S. Shafqat, "Template-Assisted Synthesis of Molecularly Imprinted Polymers for the Removal of Methyl Red From Aqueous Media," *BMC Chemistry* 17, no. 1 (2023): 46, https://doi.org/10.1186/s13065-023-01018-y.

36. J. Yang, Y. Hu, J.-B. Cai, X.-L. Zhu, and Q.-D. Su, "A New Molecularly Imprinted Polymer for Selective Extraction of Cotinine From Urine Samples by Solid-Phase Extraction," *Analytical and Bioanalytical Chemistry* 384 (2006): 761–768, https://doi.org/10.1007/s00216-005-0240-2.

37. S. Li, S. Cao, M. J. Whitcombe, and S. A. Piletsky, "Size Matters: Challenges in Imprinting Macromolecules," *Progress in Polymer Science* 39, no. 1 (2014): 145–163, https://doi.org/10.1016/j.progpolymsci.2013.06.004.

38. M. G. Mayor, G. P. González, R. G. Martínez, P. F. Hernando, and J. D. Alegría, "Synthesis and Characterization of a Molecularly Imprinted Polymer for the Determination of Spiramycin in Sheep Milk," *Food Chemistry* 221 (2017): 721–728, https://doi.org/10.1016/j.foodchem.2016.10.040.

39. M. Shekari, S. Moghari, E. A. Dawi, and H. A. Khonakdar, "Molecularly Imprinted Polymers for Diagnosis and Medical Applications: Recent Advances and Progress," *Polymers for Advanced Technologies* 36, no. 8 (2025): e70293, https://doi.org/10.1002/pat.70293.

40. M. Esfandyari-Manesh, M. Javanbakht, F. Atyabi, A. Badiei, and R. Dinarvand, "Effect of Porogenic Solvent on the Morphology, Recognition and Release Properties of Carbamazepine-Molecularly Imprinted Polymer Nanospheres," *Journal of Applied Polymer Science* 121, no. 2 (2011): 1118–1126, https://doi.org/10.1002/app.34088.

41. S. Liang, J. Wan, J. Zhu, and X. Cao, "Effects of Porogens on the Morphology and Enantioselectivity of Core–Shell Molecularly Imprinted Polymers With Ursodeoxycholic Acid," *Separation and Purification Technology* 72, no. 2 (2010): 208–216, https://doi.org/10.1016/j.seppur.2010.01.025.

42. Y. J. Qi, N. Perveen, and N. H. Khan, "Comparative Purity Study of UV Spectrophotometric and Fourier-Transform Infrared Spectroscopic (FTIR) Techniques for the Determination of Ciprofloxacin Hydrochloride Tablets," *Biological Journal of Science and Technology Research* 32, no. 3 (2020): 24973–24987, https://doi.org/10.18034/bjstr.v32i3.24987.

43. J. J. BelBruno, "Molecularly Imprinted Polymers," *Chemical Reviews* 119, no. 1 (2018): 94–119, https://doi.org/10.1021/acs.chemrev.8b00211.

44. S. Azodi-Deilamia, M. Abdoussa, and S. Rezvaneh Seyedib, "Synthesis and Characterization of Molecularly Imprinted Polymer for Controlled Release of Tramadol," *Central European Journal of Chemistry* 8 (2010): 687–695, https://doi.org/10.2478/s11532-010-0067-3.

45. X. Luo, Y. Zhan, Y. Huang, L. Yang, X. Tu, and S. Luo, "Removal of Water-Soluble Acid Dyes From Water Environment Using a Novel Magnetic Molecularly Imprinted Polymer," *Journal of Hazardous Materials* 187, no. 1–3 (2011): 274–282, https://doi.org/10.1016/j.jhazmat.2011.01.053.

46. S. A. Sadeek, W. H. El-Shwiniy, W. A. Zordok, and A. M. El-Didamony, "Spectroscopic, Structure and Antimicrobial Activity of New Y(III) and Zr(IV) Ciprofloxacin," *Spectrochimica Acta, Part A: Molecular and Biomolecular Spectroscopy* 78, no. 2 (2011): 854–867, https://doi.org/10.1016/j.saa.2010.11.060.

47. H. H. Nguyen, A. Brûlet, D. Goudounèche, P. Saint-Aguet, N. de Lauth- Viguerie, and J.-D. Marty, "The Effect of Polymer Branching and Average Molar Mass on the Formation, Stabilization and Thermoresponsive Properties of Gold Nanohybrids Stabilized by Poly(N-Isopropylacrylamides)," *Polymer Chemistry* 6, no. 32 (2015): 5838–5850, https://doi.org/10.1039/C5PY00837B.

48. Y. Mao, R. Xiong, J. Tian, G. Ling, and P. Zhang, "Advances and Applications of Metal–Organic Framework/Molecularly Imprinted Polymer (MOF/MIP) for Fluorescence Detection," *Coordination Chemistry Reviews* 537 (2025): 216691, https://doi.org/10.1016/j.ccr.2025.216691.

49. N. Arabzadeh and M. Abdouss, "Synthesis and Characterization of Molecularly Imprinted Polymers for Selective Solid-Phase Extraction of Pseudoephedrine," *Colloid Journal* 72 (2010): 446–455, https://doi.org/10.1134/S1061933X10040062.

50. L. M. Madikizela, S. S. Zunngu, N. Y. Mlunguza, N. T. Tavengwa, P. S. Mdluli, and L. Chimuka, "Application of Molecularly Imprinted Polymer Designed for the Selective Extraction of Ketoprofen From Wastewater," *Water SA* 44, no. 3 (2018): 406–418, https://doi.org/10.4314/wsa.v44i3.08.

51. C.-M. Dai, S.-U. Geissen, Y.-L. Zhang, Y.-J. Zhang, and X.-F. Zhou, "Selective Removal of Diclofenac From Contaminated Water Using Molecularly Imprinted Polymer Microspheres," *Environmental Pollution* 159, no. 6 (2011): 1660–1666, https://doi.org/10.1016/j.envpol.2011.03.012.

52. Y. A. E. H. Ali, A. Azzouz, M. Ahrouch, A. Lamaoui, N. Raza, and A. Ait Lahcen, "Molecular Imprinting Technology for Next-Generation Water Treatment via Photocatalysis and Selective Pollutant Adsorption," *Journal of Environmental Chemical Engineering* 12, no. 3 (2024): 112768, https://doi.org/10.1016/j.jece.2024.112768.

53. F. Ofridam, M. Tarhini, N. Lebaz, É. Gagnière, D. Mangin, and A. Elaissari, "pH-Sensitive Polymers: Classification and Some Fine Potential Applications," *Polymers for Advanced Technologies* 32, no. 4 (2021): 1455–1484, https://doi.org/10.1002/pat.5184.

10991581, 2026, 2, Downloaded from https://onlinelibrary.wiley.com/doi/10.1002/pat.70526 by National Institutes Of Health Malaysia, Wiley Online Library on [08/02/2026]. See the Terms and Conditions (https://onlinelibrary.wiley.com/terms-and-conditions) on Wiley Online Library for rules of use; OA articles are governed by the applicable Creative Commons License